Uncertainty in PV Module Measurement - Part I: Calibration of Crystalline and Thin Film Modules

Daniela Dirnberger, Ulli Kräling

Abstract— **This article presents recent progress in reducing the measurement uncertainty for crystalline silicon (c-Si) and thin film PV modules. It describes the measurement procedure and the uncertainty analysis as applied in CalLab PV Modules, Fraunhofer ISE's laboratory for module measurements. The uncertainty analysis covers the complete calibration process in detail, including measurements, correction to STC, and determination of electrical module parameters (I_{SC}, P_{MPP}, V_{OC} etc.) from the I-V curve. Differences between c-Si and thin film modules are addressed, most importantly in terms of spectral mismatch factor and short timescale stability problems. The paper outlines the importance of a comprehensive quality assurance system in a calibration laboratory as a prerequisite for accurate measurements on a daily basis. Particular attention is paid to results from a series of measurements taken every three weeks over a 3 year period, conducted as part of the quality assurance system. In conclusion, this article introduces a best-case uncertainty for c-Si module calibration of 1.6% for P_{MPP} and 1.3% for I_{SC}. This represents the lowest reported uncertainty for full size module calibration in a laboratory so far. The presented uncertainty in P_{MPP} of cadmium telluride and single junction amorphous silicon modules is 2.9%, and 1.8% respectively. All mentioned uncertainties are expanded uncertainties (k=2).**

Index Terms—**measurement uncertainty, calibration, crystalline silicon, thin film, I-V curve, pulsed solar simulator**

I. Introduction

Reducing measurement uncertainty has always been a major goal for scientists and metrologists in various disciplines. In the field of photovoltaics (PV), this is particularly of interest for scientists developing new cell concepts, and investors in PV systems. Specifically, the lower the uncertainty reported with a measurement result, the more evident a scientific improvement, and the lower the financial risk inherent in an investment.

The literature reveals that the uncertainty in PV module and cell measurement has been continuously improving over the past years [1-7]. Uncertainty estimation is often presented with respect to measurements close to STC (1000 W/m², 25 °C, spectral distribution according to IEC 60904-3 [8]). In the 1980s, the scientific discussion was focused on PV cells [1, 2], rather than modules. In 2001, Whitfield and Osterwald published an uncertainty analysis resulting in 1.9% for outdoor module measurements near STC [7]. Müllejans et al. published a comprehensive uncertainty analysis which also covered indoor calibration of PV modules in 2009 [3]. In this publication, the best-case uncertainty in power is reported as 1.96% for modules with less than 2 m in diagonal. Also in 2009, Emery reported 3.9% for areas up to 150 x 120 cm² [4]. Along with the results of an Asian round robin between nine laboratories, uncertainties in the range of roughly 1.8% to 5.5% are presented in [9]. The results are comparable within uncertainty limits, but no details on the uncertainty estimations are reported. Typical uncertainty values for module or submodule efficiency presented in the solar cell efficiency tables are in a range of 2-3.5% depending on the size and technology of the device [10]. The uncertainty tends to be higher for thin film technologies, and larger devices. Note that details of the uncertainty calculations cited above can differ, as the accepted rules for uncertainty estimation were still being developed.

In this article, we present recent progress in reducing the uncertainty for calibration of crystalline (c-Si) and thin film modules. In March 2010, the lowest possible uncertainty for c-Si modules was reduced to 2.0% in CalLab PV Modules [5], and is now further decreased to 1.6%. This is the outcome of continuous improvements, which have allowed for the reduction of conservative uncertainty estimates.

Stability problems especially of thin film modules are excluded as far as possible here, but are discussed in a second part of this work [11].

II. Methodology

A. Measurement Equipment

Of the three different pulsed solar simulator systems in use in CalLab PV Modules, this paper describes the system used for high precision measurements. Having been in operation for eight years, this system is the best optimized and understood.

The simulator itself is a Pasan 3b sun simulator with class AAA according to IEC 60904-9 [12], with a flash duration of 11.8 ms. 9.8 ms thereof are usable for measurement. During

Manuscript received December 19, 2012, revised February 23 and April 6, 2013; accepted April 22, 2013.

Daniela Dirnberger and Ulli Kräling are with the Fraunhofer Institute for Solar Energy Systems ISE, CalLab PV Modules, 79110 Freiburg, Germany. (phone: +49-761-4588-5758;e-mail: daniela.dirnberger@ise.fraunhofer.de).

this period, the flash is on a stable level with a temporal non-uniformity of 0.3% [12]. Spatial non-uniformity of less than 1% is obtained for module sizes less than 2.2 x 1.1 m². The distance between simulator and module plane is 8 m.

The complete measurement system is located in an air-conditioned room with an ambient temperature of 25±1 °C. Influences from stray light and reflection are minimized by black walls and tunnel intersections (apertures) along the optical axis. Irradiance is measured with a reference cell manufactured by Fraunhofer ISE and designed according to WPVS [13, 14] with an internal Pt100 temperature sensor and an external precision shunt resistor. Module temperature is measured by four Pt100 temperature sensors attached to the back of the module. 10 bit A/D converters route the temperature signals to the data acquisition (DAQ). Temperature is taken once at the beginning of each I–V curve measurement. The DAQ system (halm cetis PV-CT-L1) logs irradiance, module current, and voltage in parallel (up to 500 data points per measurement) by means of three 16 bit A/D converters. The measurement is triggered by the software, in which care is taken to use only the stable part of the flash for the measurement. The electronic load sweeps the I–V curve through two quadrants (i. e. no negative currents occur). Voltage and current are measured with four-wire technology in a maximum range of ±250 V and ±20 A respectively. The DAQ system and electronic load are capable of both hysteresis and section measurements for controlling voltage sweep rate related capacity effects. Hysteresis measurements are measurements from I_{SC} to V_{OC} (forward) and V_{OC} to I_{SC} (backward). This allows for the detection of module capacity related over- or underestimations in the module power by calculating the hysteresis (Equation 1) between forward and backward measurement ([5], compare also [15]).

$$hyst = \frac{P_{MPP,backward} - P_{MPP,forward}}{P_{MPP,backward} + P_{MPP,forward}} * 100\% \qquad (1)$$

If the hysteresis is larger than desired, the voltage sweep rate per flash can be decreased by section measurements. For a section measurement, the I−V curve is not measured entirely during one flash, but is swept in smaller voltage sections during several flashes (compare [16]).

B. *The Quality Assurance System and Traceability Chain*

The quality assurance system includes three important components. First, regular measurements of PV modules to assure constant system performance are carried out. These measurements are performed for three timescales:

- International round robin tests on a yearly basis, to compare different traceability chains and measurement methods. CalLab PV Modules took part in round robin tests presented in [17-19] and organized the tests mentioned in [20, 21].
- Quality assurance measurements every three weeks, performed on the same set of modules in all simulators, the aim being to detect long-term drifts and differences between the simulators.

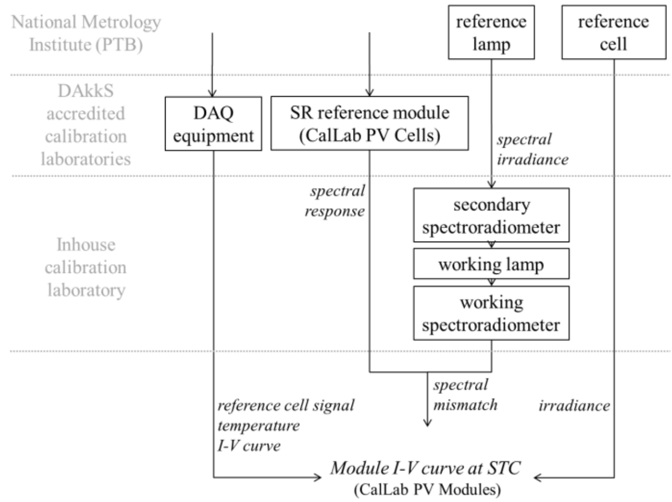

Fig. 1. Traceability chain of CalLab PV Modules with regard to the calibration of measurement equipment (boxes) and traceability of measured quantities (italic).

- Daily quality assurance measurements at the beginning and the end of each working day, performed on one module per system. The aim is to detect equipment malfunctions immediately, as well as drifts within three weeks.

Second, all measurement equipment in use is recalibrated once a year. The full traceability chain is depicted in Fig. 1. All electrical equipment and all temperature sensors are calibrated by DAkkS[1] accredited laboratories. All reference cells are primary calibrated by PTB[2] [22-24]. The calibration is thus traceable to SI units. Worldwide, different methods for primary cell calibration exist that were compared several times in the past [14, 25, 26].

Third, measurement tools developed in-house are used for testing simulator characteristics. The relative spectral distribution of the simulator is measured with a calibrated spectroradiometer traceable to PTB. The instrument is a single monochromator diode array spectroradiometer. The complete sensor unit consists of three diode arrays, together covering a wavelength range of 280-1700 nm.

More details on this instrument and the measurement of the spectral distribution of a pulsed solar simulator are reported in [6, 27]. The spectral distribution is measured every week, in order to keep track of spectral changes due to lamp ageing. With increasing number of flashes performed with a lamp, the NIR share of the spectral distribution increases, while the UV share decreases. The magnitude of that change depends on the quality of the lamps and must therefore be monitored carefully, as it affects the spectral mismatch factor (*MM*).

Spatial non-uniformity is also regularly checked. This is especially important to verify the position of the reference cell, which must be at a place of average irradiance [28]. The measurements are conducted by means of a specially designed

[1] DAkks: German accreditation body
[2] PTB: Physikalisch-Technische Bundesanstalt, the national metrology institute of Germany

module with 4x12 cells for non-uniformity measurements. The short circuit current and temperature of each cell are measured in parallel, thus providing a quick and reliable way to examine non-uniformity of irradiance.

The importance of the quality assurance system with regard to measurement uncertainty is to verify periodically whether the current situation is in compliance with set limits, and to trigger interventions in case of malfunctions. It can also aid in the investigation and quantification of currently inexplicable effects (mostly: deviations from expected measurement results). Uncertainty is a value that “expresses how well one believes to know the essentially unique true value of the measurand” according to GUM ([29], page 3). Based on that, a sophisticated quality assurance system can decrease uncertainty, as the analytically unknown contributions to uncertainty can be estimated within smaller limits, i.e. less conservatively as would be necessary without the knowledge from regular measurements.

C. Measurement Procedure

Our measurement procedure follows the recommendations given in IEC 60904 [8, 28, 30, 31].

The reference cell is mounted in the module plane, the position having been decided in accordance with the results from non-uniformity measurements, in order to ensure that the reference cell measures the average irradiance in module plane [28]. The simulator irradiance is set to the level for which the reference cell including *MM* indicates 1000 W/m². The aim is to perform the measurement with an “effective irradiance” (i. e. the irradiance that actually contributes to photocurrent generation in the device under test) as close as possible to 1000 W/m², so that the device under test will produce the same photocurrent as at STC.

The spectral mismatch correction is based on the spectral response (SR) of a module of the same type and batch as the module under test. The SR of one cell of this SR reference module is measured by CalLab PV Cells, Fraunhofer ISE’s laboratory for cell measurements which is accredited by DAkkS. The relative spectral distribution of the simulator is available from the weekly measurements.

For each module under test, three hysteresis measurements are taken. If necessary, section measurements are performed so that the hysteresis according to Equation 1 is less than 0.5%. The obtained raw data is evaluated with an in-house developed software based on the script programming language python [32]. The software is used for evaluation of I−V curves from all three simulators. It corrects the I-V curve to STC point-by-point, and with regard to temperature and irradiance, by means of a procedure comparable to IEC 60891 [33]. The software averages forward and backward curves, and determines the electrical module parameters (I_{SC}, I_{MPP}, P_{MPP}, V_{MPP}, V_{OC}, *FF* and efficiency) from the averaged I−V curve. The averaging is done point-by-point after interpolation of the forward and backward curves to the same voltage values. I_{SC} and V_{OC} are determined by linear fits to selected voltage or current ranges, respectively, of the I−V curve. A 5th order polynomial fit is applied to a selected voltage range of the P−V curve in the case of P_{MPP}. A sophisticated algorithm suitable for all types of modules was developed for this purpose. The final measurement result is the average of the electrical module parameters obtained from the three hysteresis measurements.

D. Contributions to Uncertainty

Fig. 2 summarizes the most important contributions to uncertainty with regard to the measurement and evaluation process, and outlines where, how and why exactly uncertainty is introduced and propagated. The measurement process itself consists of the determination of irradiance and temperature as well as the module’s I−V curve. Stability problems will be addressed briefly only for thin film modules. For c-Si modules that are being calibrated, one should make sure that light induced degradation has already taken place [34].

The evaluation process consists of two main steps which both carry uncertainty: First, the measured I−V curve is corrected to STC, using the determined effective irradiance

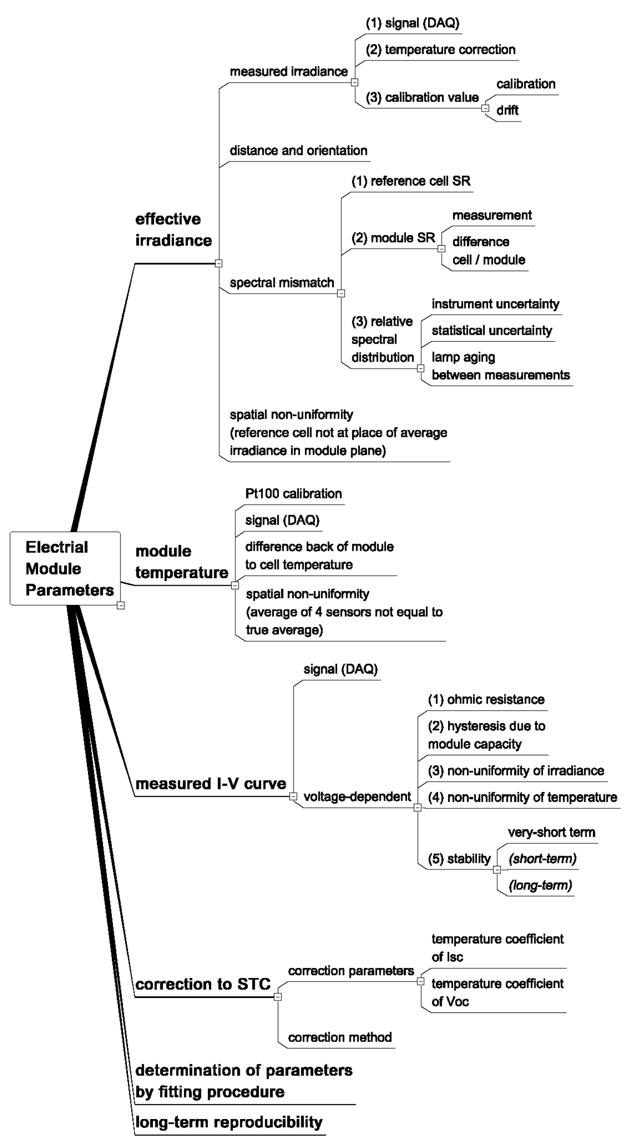

Fig. 2. Sources of Uncertainty

and measured temperature. Second, the electrical module parameters are derived from the corrected I−V curve.

E. Uncertainty Estimation

The uncertainty estimation presented in the following was performed according to the rules stated in the “Guide to the expression of uncertainty in measurement” [35, 36], henceforth referred to as GUM. Very briefly summarized, the necessary steps for evaluating and expressing the uncertainty of a measurement result, as presented in GUM’s chapter 8, are: (1) A measurement equation that expresses the relation between measurand and input quantities must be formulated. Estimated values of (2) input quantities must be determined along with (3) their standard uncertainty and (4) their possible correlations. (5) The result of the measurement is to be calculated using the measurement equation. (6) The combined standard uncertainty must be determined from the standard uncertainties of, and correlations between, the inputs to the measurement equation. (7) The expanded uncertainty must be given, and (8) the measurement result must be presented along with the combined standard or expanded uncertainty.

The goal pursued here is to establish an uncertainty calculation based on an as well as possible standardized procedure, in order to enable the easy adaption to other measurement systems. Furthermore, the procedure should allow for the direct use of relative uncertainties, as it is intended to be valid for the majority of existing PV modules. Uncertainty estimations for fitting and correction procedures, which complicate the strict use of GUM, should be includable easily. As a consequence, some simplifications compared to the strict application of GUM are necessary, which are described in the following.

Comprehensive analytical measurement equations are not used here, as the relation between all input quantities and the measurement result cannot be expressed in an analytical equation with current knowledge. Instead, we use the simplification suggested in paragraphs 5.1.4 and 5.1.5 of GUM. The measurement equation (Equation 2) expresses empirically how a certain change in an input quantity X_i propagates to the output quantity Y.

$$Y = Y_0 + c_1\delta_1 + c_2\delta_2 + \cdots + c_\mathrm{n}\delta_\mathrm{n} \tag{2}$$

with Y being the measurand, X_i the input quantities, $Y_0 = f\left(X_{1,0}, X_{2,0}, \ldots, X_{\mathrm{n},0}\right)$ and $X_{1,0}, X_{2,0}, \ldots, X_{\mathrm{n},0}$ nominal values, $\delta_\mathrm{i} = X_\mathrm{i} - X_{i,0}$ transformations of the input quantities, and c_i the sensitivity coefficients.

Details on the estimation of relevant values for input quantities and their standard deviation are presented in section III. All uncertainties presented in the tables are relative standard uncertainties unless explicitly stated otherwise. Occasionally, the half width of a rectangular probability distribution will be given in the text, which is indicated by ‘±’ preceding the number. The standard uncertainty of a rectangular probability distribution with half width a is $a/\sqrt{3}$.

As Equation 2 still represents a theoretical construct, the measurement result is not calculated using the measurement equation, but determined by the steps described in section II.C. The combined uncertainty is calculated according to the law of propagation of uncertainty (equation 10 in GUM) as follows:

$$u_\mathrm{c}^2(y) = (c_1 u_{\mathrm{X1}})^2 + (c_2 u_{\mathrm{X2}})^2 + \cdots + (c_n u_{\mathrm{Xn}})^2 \tag{3}$$

Combined uncertainties for all the nodes in Figure 2 can be calculated repetitively using Equation 3, and can therefore stand for the combined uncertainty for measured irradiance, effective irradiance and lastly I_SC, P_MPP, etc. This allows for a relatively simple and standardized calculation of uncertainty. One must be aware that, by proceeding alike, all input quantities are treated as uncorrelated. This approximation is possible as correlations between input quantities are assumed to be negligible. This will be addressed in a little more detail below with regard to P_MPP and FF.

The sensitivity coefficients c_i are determined empirically; i. e. experimentally based on measurements, or measurements on similar objects (GUM paragraph 5.1.5). Very often, c_i are unity, meaning that the determined uncertainty of the input quantity X_i fully propagates to Y. This is especially the case when uncertainty of X_i is estimated directly in the units of Y, e. g. in the case of all contributions to uncertainty of irradiance, temperature and I-V curve (see Tables I, II and III). However, with regard to the propagation of uncertainty in irradiance to voltage and current, different sensitivity coefficients need to be applied as current is directly proportional to irradiance, whereas voltage is not. Details are given in section III.

The expanded uncertainty of all electrical module parameters is calculated with a coverage factor k=2, in order to obtain a 95% coverage interval. We consider the probability distribution of the measurement result to be normal, as a significant number of input quantities with normal and rectangular distributions are involved (see G.6.6 of GUM).

III. Results of Uncertainty Estimation

A. Uncertainty Estimation for c-Si Modules

In this section, we will explain the sources of uncertainty considered in Fig. 2 more closely and present our quantitative estimations. The results hold true for standard c-Si modules (i. e. no stability problems, no special sweep rate sensitivity), measurement with spectral mismatch correction at STC and module sizes up to 2.2 x 1.1 m².

Effective Irradiance

The “effective irradiance” differs from the irradiance measured by the reference cell in terms of distance from and orientation to the light source, the spectral mismatch factor *MM*, and spatial non-uniformity.

The uncertainty of measured irradiance is composed of the following four contributions (see also Table I and Fig. 2, note the numbering intended to match text and figure): (1) The

TABLE I
CONTRIBUTIONS TO UNCERTAINTY OF EFFECTIVE IRRADIANCE

Source	Relative standard uncertainty in %	Probability distribution
Signal (DAQ)	0.059	normal
Temperature correction	0.011	normal
Calibration	0.300	normal
Drift	0.115	rectangular
Distance/orientation	0.084	rectangular
Spectral Mismatch	0.420	normal
Spatial non-uniformity (offset)	0.173	rectangular
Combined relative standard uncertainty in %	0.566	normal

Results of the uncertainty estimation for irradiance, valid for quantity values of 1000±10 W/m². The underlying spatial non-uniformity is 0.84%. The combined uncertainty is calculated according to Equation 3 with c_i being unity.

uncertainty introduced by the complete acquisition chain of the reference cell signal is 0.059% (including the shunt resistor). (2) The uncertainty due to temperature correction is estimated to be 0.011%, based on the prerequisite that temperature in the laboratory and thus of the reference cell is 25±1 °C. (3) The expanded uncertainty of the calibration value provided by PTB is 0.6% (k=2) [24]. Currently, this is the worldwide lowest uncertainty for reference cell calibration. The maximum drift is considered to be ±0.2%. This is based on our experience from yearly recalibrations at PTB. Non-linearity can be neglected for STC measurements, because the PTB calibration report states excellent linearity near 1000 W/m² (deviation less than 0.001%).

With regard to distance from and orientation to light source, only the module frame itself can cause uncertainty, as reference cell and module are mounted to a rigid and well aligned structure. The maximum distance error is estimated to be ±5 mm, the maximum non-parallelism error to be ±2.5 mm. This results in an uncertainty of 0.084%, assuming a point source of light (which is an approximation; see also [3]).

To estimate the uncertainty of the *MM* is a challenge of its own [37-39]. It must include the uncertainties of reference cell and module SR, respectively, as well as the relative spectral distribution of the light source. We estimated the uncertainty with a similar, but somewhat more conservative Monte Carlo approach [40] as proposed in [38]. The approach in [38] estimates the uncertainty of a *MM* by calculating the *MM* from 10000 representations of the input data set. These representations are created by means of a set of 10000 normalized random walks (RW). The RW are cumulated sum vectors calculated from a set of random number vectors, the elements of which were drawn from a normal standard distribution. The normalization is done in [38] by dividing all RW by their respective maximum values, i. e. so that the maximum is unity. We use a wavelength-dependent normalization which ensures that, for each wavelength, the standard deviation of the values of all RW is equal to the estimated relative standard uncertainty of SR and spectral irradiance. This improves the sensitivity of the simulation to input data uncertainty and, for uncertainties determined in the following, tends to increase the *MM* uncertainty compared to results in [38].

(1) The uncertainty of reference cell SR is provided by the PTB calibration report, and is less than 0.5% between 300-1000 nm. (2) The combined uncertainty of the module SR includes two contributions (Fig. 3): First, the measurement uncertainty itself is provided by CalLab PV Cells. Note that the uncertainty for measurement of cells within a module is higher than for individual cells because temperature control is more difficult[3]. Second, uncertainty due to the difference of SR of the measured cell (of the SR reference module) and the whole module under test is estimated from the standard deviation observed from measurements of 20 typical c-Si cells. (3) The combined uncertainty of spectral distribution is calculated from three contributions (Fig. 4): the estimated measurement uncertainty from analyzing the spectroradiometer presented in [6], the average standard deviation from 5 measurements (the weekly measurement is the average of 5 measurements), and the standard deviation of the change due to lamp ageing from week to week.

Data from January to April 2012 were analyzed in order to quantify standard deviation and weekly change. As the

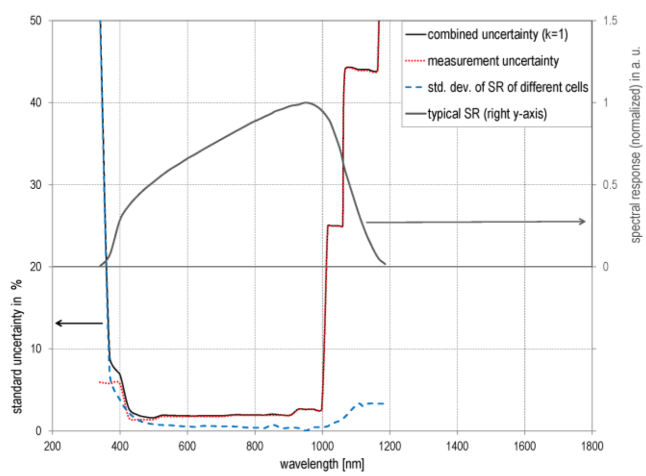

Fig. 3. Uncertainty of spectral response of a typical c-si module.

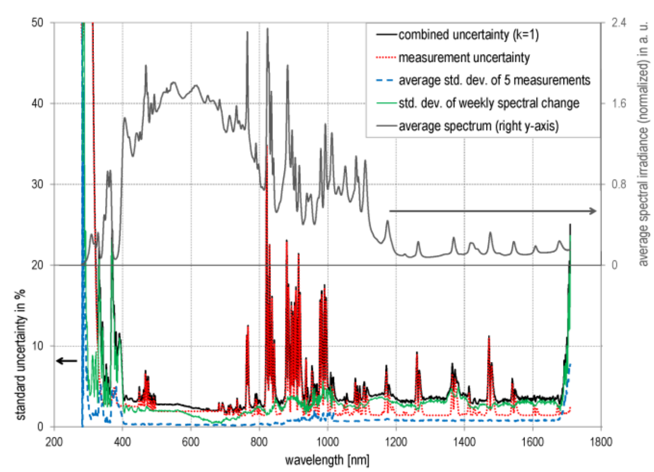

Fig. 4. Uncertainty of spectral distribution used for spectral MM correction.

[3] personal communication, Jochen Hohl-Ebinger, Fraunhofer ISE

spectral distribution of the simulator, and thus the *MM*, is dependent on larger changes of the lamp voltage, it is important to note that all considered measurements of the spectral distribution were performed very close to the 1000 W/m² level (i. e. with lamp voltages equal to those during a normal STC measurement). The resulting uncertainty of the *MM* is 0.420% for a typical c-Si module measured with a typical Fraunhofer ISE reference cell (e. g. as depicted in [38]).

The spatial non-uniformity is 0.84%, determined with the above-mentioned non-uniformity device and calculated according to Equation 4 [12].

$$non\ uniformity = \frac{G_{\max}-G_{\min}}{G_{\max}+G_{\min}} * 100\% \qquad (4)$$

It contributes to measurement uncertainty in two ways: First, the existence of dark and bright spots leads to different photocurrents in the different cells and affects the shape of the I-V curve [41]. This contribution is considered separately below in section “Module I-V curve”. Second, and more importantly, a bias error can occur if the reference cell sits on an especially bright spot in the plane of measurement. In order to minimize this bias, the cell is placed at a spot with irradiance equal to the average irradiance in module plane [28]. It is important to note that uncertainty remains, as the selection of this spot is still not exact. This is due to the measurement uncertainty inherent in the non-uniformity determination, and the size difference of reference cell and the cells of the non-uniformity device. The remaining uncertainty is estimated with regard to the non-uniformity in the immediate surroundings of the selected spot, the measurement being performed with a device of the same size as the reference cell. The determined non-uniformity is 0.3%, which is considered as an uncertainty with a rectangular probability distribution.

The combined uncertainty in the effective irradiance results in 0.566% for irradiance levels close to 1000 W/m².

Note that the influence from temporal non-uniformity is negligible, as long term stability as defined in IEC 60904-9 is better than 0.3%, and the correction to 1000 W/m² is done point-by-point. As a consequence of this very stable operation of the flash lamp within one pulse, the spectral distribution does not change considerably while the pulse is on its stable plateau [27].

Module Temperature

The uncertainty introduced by module temperature measurement is combined from sensor calibration, the unknown temperature difference between module backside and p-n junction, and temperature non-uniformity (Table II). As a requirement for the measurement, the temperature of each of the four sensors must be within 25±1 °C, which results in a maximum non-uniformity of temperature of 4%.

Information on uncertainty introduced by the temperature sensor is obtained from the calibration report (offset tolerance: ±0.1 K at maximum). The DAQ uncertainty, including measurement and resolution, is 0.327%. As the module is stored in a temperature controlled environment several hours before the measurement, we assume the difference between backside and p-n junction to be less than ±0.1 K, which results in an uncertainty of 0.231%. The effects of spatial non-uniformity of temperature are, in general, similar to that described for irradiance: there is an offset uncertainty, and an effect on I−V curve that will be discussed below. The maximum difference of the true average temperature and the average of the four sensors is estimated to be less than ±0.1 K as a consequence of the storage of the module. The uncertainty in module temperature results in 0.517% for temperature levels close to 25 °C.

TABLE II
CONTRIBUTIONS TO UNCERTAINTY OF TEMPERATURE

Source	Relative standard uncertainty in %	Probability distribution
Temperature sensor (Pt100 calibration)	0.231	rectangular
Signal (DAQ)	0.327	normal
p-n-junction / backside	0.231	rectangular
Temperature non-uniformity (offset)	0.231	rectangular
Combined relative standard uncertainty in %	0.517	normal

Results of the uncertainty estimation for temperature, valid for quantity values of 25±1 °C. The underlying estimated spatial non-uniformity is 4%. The combined uncertainty is calculated according to Equation 3 with c_i being unity.

Module I−V curve

The uncertainty of the measured I−V curve is composed of DAQ contributions for each point, and a voltage-dependent contribution which affects the shape of the I−V curve (Fig. 2 and Table III). All standard uncertainties are estimated with regard to a specific electrical module parameter. Unless otherwise specified, the uncertainty for P_{MPP} and *FF* is the root sum of squares of I_{MPP} and V_{MPP}, or I_{SC}, V_{OC}, and P_{MPP} respectively. Correlations are assumed to be negligible.

Contributions to DAQ uncertainty sum up to 0.058% both for current and voltage.

In terms of voltage-dependent uncertainty, we consider ohmic resistance, voltage sweep rate related capacity effects that cause hysteresis, the propagation of irradiance and temperature non-uniformity and stability related effects (Fig. 2, note numbering). (1) Ohmic resistance before the four wire measurement point introduces current-dependent voltage drops, i. e. offsets to the true voltage. This affects neither V_{OC} (no current), nor the current measurement itself, i. e. I_{SC} and I_{MPP}. The maximum resistance is estimated to be 2 mOhm (roughly 10 cm cable from module connectors to four-wire-measurement point). In MPP, 2 mOhm cause a voltage shift of 16 mV, assuming a maximum current of 10 A. This results in a relative uncertainty of 0.058% for V_{MPP} and P_{MPP} (even though this is a directed uncertainty, we consider this in both directions for simplicity). (2) Uncertainty due to voltage sweep rate related capacity effects is minimized by section and hysteresis measurements. The maximum accepted

TABLE III
CONTRIBUTIONS TO UNCERTAINTY OF I-V CURVE PARAMETERS FOR C-SI MODULES

Relative standard uncertainty in %	I_{SC}	I_{MPP}	V_{OC}	V_{MPP}	P_{MPP}	FF	Probability distribution
Signal (DAQ)	0.058	0.058	0.058	0.058	0.082	0.117	rectangular
Ohmic resistance	0.000	0.000	0.000	0.058	0.058	0.058	rectangular
Hysteresis	0.115	0.128	0.192	0.377	0.289	0.366	normal, except P_{MPP} rectangular
Irradiance Non-Uniformity	0.058	0.058	0.035	0.035	0.067	0.095	rectangular
Temperature Non-Uniformity	0.023	0.023	0.191	0.191	0.192	0.271	rectangular
Very-short-term stability	0	0	0	0	0	0	rectangular
Combined relative standard uncertainty in %	0.144	0.154	0.279	0.431	0.367	0.483	normal

Results of the uncertainty estimation for the parameters of the measured I-V curve, valid for values of typical commercially available modules. The combined uncertainties were calculated according to Equation 3 with c_i being unity for each column. In the columns for P_{MPP} and FF, the standard uncertainty in each line is the root sum of squares of I_{MPP}, $V_{MPP;}$ or I_{SC}, I_{MPP}, V_{OC}, $V_{MPP,}$ respectively; except for hysteresis (P_{MPP}) and irradiance non-uniformity (P_{MPP} and FF),where the standard uncertainty was estimated directly.

hysteresis in MPP (Equation 1) is 0.5%. This ensures that the true power never differs more than ±0.5% from the P_{MPP} determined from the averaged I-V curve. This maximum error is considered in the uncertainty estimation. As the deviation of forward and backward curve from the true curve is not necessarily symmetrical [41], the probability distribution is considered rectangular This results in a standard uncertainty due to hysteresis of 0.289% in P_{MPP}. Apart from P_{MPP}, we found from comparisons of several forward and backward I−V curves that an influence on I_{SC} and V_{OC} cannot be excluded. We estimated uncertainty as presented in Table III from this comparison. It must be stated that at this stage in the analysis, it is not possible to clearly separate DAQ and data-handling-related (random) uncertainties from actual hysteresis (systematic) uncertainties. Therefore, the attributed uncertainty due to hysteresis might be overestimated.

As mentioned above, the non-uniformity of irradiance and temperature has an additional influence on the I−V curve. In the case of irradiance (3), we estimated the influence based on a simulation. For a typically designed module (6x10 Cells, 3 bypass diodes) and different non-uniformity profiles, the deviation of resulting electrical module parameters compared to perfect uniformity was calculated. The underlying simulation model was presented in [42]. For a typical 2% non-uniformity profile, the simulation calculated a deviation in FF of roughly +0.2%. Based on our non-uniformity of 0.84%, we conservatively estimated the standard uncertainty for all electrical module parameters as given in Table III. The effect of temperature non-uniformity (4) is estimated by multiplying the maximum non-uniformity of 1 K (4% of 25 °C) with the temperature coefficients. As temperature coefficients, we used technology specific best estimates from a large data set obtained throughout the past years: −0.33%/K for V_{OC} and as approximation for V_{MPP}, 0.04%/K for current values respectively. Possible correlations are neglected because their impact is limited owing to the strict temperature limits. (5) Stability effects do not need to be considered for standard c-Si technologies.

Correction to STC and Parameter Determination

Even though the limits for deviations from STC are set very tight (1000±2 W/m², 25±1°C for the average of all measurement points), there is a contribution to uncertainty from correction to STC. It must be considered that the correction parameters are never known exactly. The uncertainty of the temperature coefficient is estimated to be ±0.1 %/K for voltage, and ±0.02 %/K for current (see also [43]). The contribution to uncertainty due to correction for all electrical module parameters was estimated by varying the correction parameters and methods, and is presented in Table IV. The uncertainty of I_{MPP}, V_{MPP} and P_{MPP} is a magnitude higher compared to I_{SC} and V_{OC}.

The uncertainty inherent in determination of electrical module parameters by fitting is estimated by varying the algorithm and the range of data used for the fit. The uncertainty might be overestimated in both cases, as DAQ and actual data evaluation uncertainty superimposes.

Reproducibility Factor

We mentioned above that "uncertainty is a measure to describe how well one believes one knows" [29] the true value of a measurand. Relating this to the process of uncertainty estimation, it must be concluded that a consistently optimistic uncertainty estimation without good reason might be an overestimation of one's knowledge. The presented uncertainty analysis is comprehensive inasmuch as it covers all important contributions. However, it still contains neglected correlations, and some, however small, contributions that are to date unsatisfactorily quantified or that cannot be detected immediately by the quality assurance system. Furthermore, it does so far not consider the possible influence from the operator performing the measurement, even though this influence is small as measurements are performed according to recognized guidelines. To account for this, we include an additional "reproducibility factor" from our 3-weekly quality assurance measurements. This is not a first order implication from applying GUM, but is a practical solution for expressing the "degree of belief".

The reproducibility factor is obtained from measurements of a set of nine modules (c-Si, different sizes and manufacturers). Data measured since January 2010 was used (3 modules only since end of 2010). Fig. 5 shows a boxplot of the deviation of power from the long-term module-specific average (left), and the distribution of that deviation for all

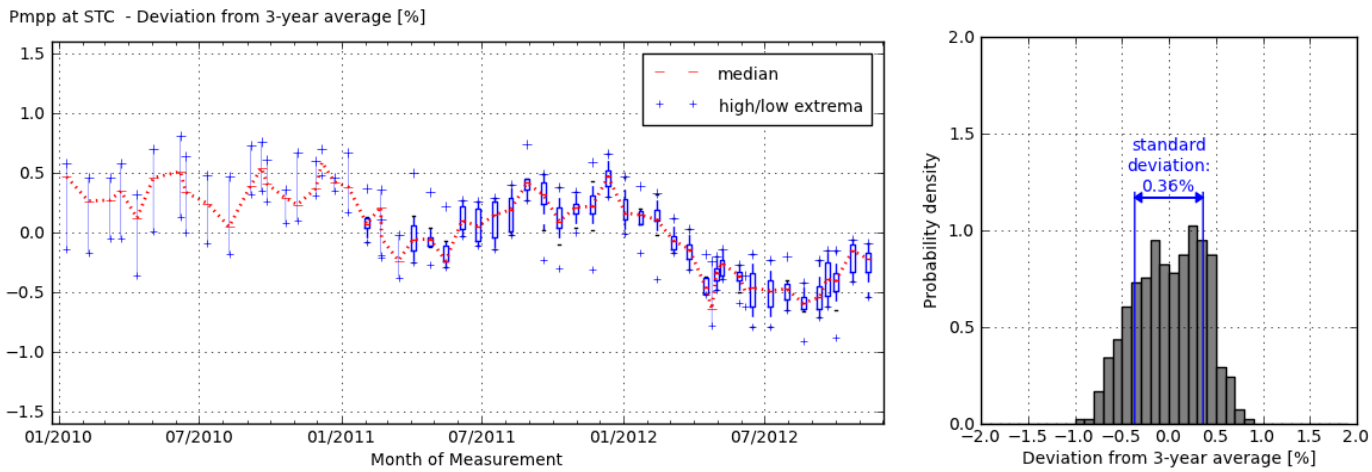

Fig. 5. Long-term reproducibility for module power in CalLab PV Modules since 2010. For 9 modules (6 before 2011) used for 3-weekly quality assurance measurements, the deviation in percent from module average is depicted vs. time (left). The distribution of this deviation for all modules and measurements is displayed on the right. The standard deviation of this distribution is taken as an additional contribution to uncertainty.

measurements (right). The supposed obvious trend is in fact mainly due to the use of different reference cells with individual uncertainty, overlaid by usual scatter. The cell used from March to May 2011 and from March 2012 until now shifts measurement results below the level obtained with different cells used before. The shift is well within the uncertainty of the calibration value.

The single standard deviation calculated with the data in Fig. 5 is considered in the uncertainty estimation as the reproducibility factor. Table IV summarizes the results for all parameters.

Calculation of combined and expanded uncertainty

Table IV presents a summary of all discussed contributions to uncertainties in the electrical module parameters. The resulting combined uncertainties were calculated according to Equation 3. Possible correlations are assumed to be negligible. An explanation for this assumption is given in the following for the most obviously possible correlations due to temperature and irradiance. Note that the reasoning is intended for irradiance values close to 1000W/m², and small temperature changes only. In the case of P_{MPP}, both I_{MPP} and V_{MPP} depend on irradiance. As I_{MPP} is directly proportional to irradiance and voltage is logarithmically dependent on irradiance, i. e. negligible for small changes of irradiance, neglecting the correlation is justifiable. Similarly, the dependence of I_{MPP} on temperature is very small and thus negligible. In the case of FF, the quotient of I_{MPP} and I_{SC} is independent from irradiance, and can also be assumed independent from temperature due to the small temperature coefficients. The quotient of V_{MPP} and V_{OC} can be assumed independent from irradiance, and the slightly different change with temperature of V_{MPP} and V_{OC} (due to different relative temperature coefficients) can be neglected for small changes of temperature.

The sensitivity coefficients used are unity except for the uncertainties in effective irradiance and temperature. With regard to irradiance, c_i were determined from the irradiance dependency obtained from measurements at 1000 W/m² and 900 W/m² for a variety of modules. c is unity for I_{SC} and I_{MPP}, current being directly proportional to irradiance. c is 0.06 for V_{OC} and approximately for $V_{MPP,}$ and 0.12 for FF. The contribution to uncertainty as given in Table IV is $c_i u_{Xi}$, i. e. 0.566%·c for irradiance. For temperature, c_i equals the

TABLE IV
RESULTS OF UNCERTAINTY ESTIMATION

Contribution to uncertainty $c_i u_{Xi}$ in %	I_{SC}	I_{MPP}	V_{OC}	V_{MPP}	P_{MPP}	FF
Effective irradiance	0.566	0.566	0.034	0.034	0.567	0.068
Temperature	0.005	0.005	0.043	0.043	0.043	0.061
I-V curve	0.144	0.154	0.279	0.431	0.367	0.483
Correction to STC	0.026	0.026	0.118	0.316	0.226	0.256
Fit	0.023	0.462	0.038	0.165	0.044	0.063
Reproducibility Factor	0.287	0.350	0.056	0.244	0.364	0.174
Combined standard uncertainty in %	0.651	0.825	0.315	0.613	0.802	0.584
Expanded Uncertainty (k=2)	1.3	1.7	0.6	1.2	1.6	1.2

Results of the uncertainty estimation for all electrical I−V curve parameters, valid for values of typical commercially available modules, and module size smaller than 2.2 x 1.1 m². The combined uncertainties were calculated according to Equation 3 for each column. In the columns for P_{MPP} and FF, the standard uncertainty in each line is the root sum of squares of I_{MPP}, V_{MPP} or I_{SC}, I_{MPP}, V_{OC}, V_{MPP} respectively (exceptions: Correction to STC and Fit (P_{MPP}), Reproducibility Factor (FF and P_{MPP}). Sensitivity coefficients c_i are unity except for irradiance and temperature (see previous page for c_i values).

temperature coefficients (−0.33%/K and 0.04%/K) times the reference temperature of 25 °C.

B. *Considerations for Thin Film Technologies*

The uncertainties discussed above apply to thin film technologies as well, but some points need an adjustment in magnitude of the influence.

Spectral Mismatch Factor (MM)

According to our uncertainty estimation procedure, the magnitude of *MM* is not necessarily correlated with the magnitude of its uncertainty (in contrary to [37]). It is more important that reference cell and module have similar band edges [38]. For cadmium telluride (CdTe) modules, a typical *MM* value for measurements with a c-Si reference cell is 1.003±1.5%, and with a KG3 filtered reference cell 1.041±1.1%. We have shown in [21] that actual measurement results reflect this by a better reproducibility when using a KG3 filtered reference cell. This forms our standard procedure. Compared to c-Si, the uncertainty of *MM* is relatively high for CdTe (1.1% compared to 0.42%). This is due to the fact that we use a standard SR for correction, and no module-specific measured SR. We estimated the uncertainty from all available CdTe SR data, and naturally this results in a relatively high uncertainty. The uncertainty of effective irradiance is 1.175% for CdTe instead of 0.566%, which propagates fully to I_{SC} and P_{MPP}.

For typical amorphous silicon (a-Si), the uncertainty of *MM* is similar to c-Si if a KG3 reference cell is used, and the SR is known with a similar uncertainty. In most practical cases, the uncertainty will be somewhat higher. For the variety of different CI(G)S technologies, a specific analysis depending on the composure of the semiconductor, i. e. the manufacturer and the type, is necessary. Quantifying the uncertainty due to spectral distribution for tandem technologies, e. g. a-Si/µ-Si, is out of the scope of this paper. The spectral distribution influences the current matching of the stacked cells which can only partly, if at all, be corrected by applying *MM* [41, 44].

Spatial Non-uniformity

In our experience, spatial non-uniformity of light affects thin film modules to a lesser extent than c-Si. This practical observation is in accordance with the theoretical assumption that non-uniformity can cancel out better over the length of the long, slender cells of thin film modules than for the mostly quadratic cells of a c-Si module. However, as we have not investigated this on a quantitative basis, the same contributions to uncertainty are considered for thin film modules.

Module Temperature

Contributions to uncertainty due to temperature are estimated to be somewhat larger for glass-glass modules compared to modules with a polymeric backsheet. The maximum difference between p-n junction and backside is estimated to be ±0.3 K instead of ±0.1 K. The uncertainty of module temperature is 0.800%. As explained above, the propagation of temperature-related uncertainty is basically proportional to the temperature coefficients of a module. A-Si and CdTe modules having smaller temperature coefficients than c-Si modules, the temperature-related uncertainty for P_{MPP} etc. does not increase significantly.

Short Timescale Stability Problems

Even though stability issues are not discussed in detail here, one must be aware that “very-short-term” stability effects, i. e. effects that occur on a short timescale within milliseconds before, after or even due to the measurement, need to be considered for some thin film technologies. Difficulties can arise in separating such stability effects from sweep-speed-related capacity effects, especially when working with a pulsed solar simulator.

In [11], a very straightforward test series will be presented that investigates short timescale effects on the short-term repeatability by subsequent measurements with different delay in between the flashes. The results indicate considerable variation in the electrical module parameters for CdTe and CIS samples. Based on that, uncertainty due to small timescale stability effects is considered here as follows (rectangle limits are given): For CdTe, ±0.2% for I_{SC}, V_{OC} and *FF*, ±0.5% for I_{MPP} and V_{MPP}, and ±0.6% for P_{MPP}. For a-Si, ±0.1% for all values except V_{OC} (0%) is considered. For CI(G)S, we do not make a general conclusion due to the large variety of types.

Reproducibility Factor

For thin film modules, no history comparable to that for c-Si modules is available. However, the experience from regular thin film measurements presented in [21] permits assigning the reproducibility factor obtained for c-Si to thin film modules in principle. To account for the somewhat higher scatter in thin film measurements compared to c-Si measurement, a factor of 1.5 is applied to the single standard deviation (compare Fig. 5 right).

C. *Result and Discussion*

Table V compares expanded uncertainty for c-Si, CdTe and a-Si. The resulting expanded uncertainty for c-Si modules of 1.6% for P_{MPP} and 1.3% for I_{SC} is the lowest uncertainty for the calibration of c-Si modules reported in detail so far. For modules larger than 2.2 x 1.1 m², with pronounced sweep-speed sensitivity or other special characteristics, the analysis must be adapted.

The measurement uncertainty for CdTe and a-Si is not principally limited to specific manufacturers or module types, but it must be considered that important characteristics such as short timescale stability or SR will change with ongoing development of the technology, i. e. with manufacturer or module type. Therefore, before assigning the presented measurement uncertainty to a specific module type, especially these two characteristics should be investigated.

Potential for further reduction of the measurement uncertainty depends on the technology. For c-Si, the most important contribution is that of *MM*, followed by the uncertainty of the calibration value of the reference cell. As a consequence, a significant reduction of measurement uncertainty is unlikely without a reduction of SR uncertainty and/or uncertainty inherent in primary calibration. The uncertainty of module SR could be decreased to the usual cell SR measurement uncertainty by implementing better temperature control. This holds the potential to decrease uncertainty to 1.4% for P_{MPP}. As to the uncertainty in primary calibrations, it is not clear to date how much it is likely to be reduced in the coming years. Of course, this would affect the uncertainty for all kinds of technologies. With regard to I–V curve and STC-correction related uncertainties, ongoing research and refinement of measurement and calculation methods have minor potential for reduction. The reproducibility factor, which is also an important contribution, can be reduced only in the long run, by continuous improvement of reproducibility, or by further improving and detailing the uncertainty estimation, which could replace the use of the reproducibility factor.

For CdTe, uncertainty of *MM* is relatively high due to a large uncertainty assumed for the SR Through better characterization of the SR of the module under test, a reduction is anticipated in the near future. The second important contribution which increases uncertainty is the short timescale stability. This is likely to differ between different module generations. Therefore, whether the measurement uncertainty can be decreased is dependent upon the module behavior, as well as the development of measurement methods to reduce these instability effects.

Finally, when speaking about calibration of modules, the following must be considered: Calibration seeks to determine the electrical module parameters, e. g. to use this module as a reference for further measurement tasks. Whether the power is representative for field operation is not primarily of interest, but the stability of the module is mandatory. The required stability was observed for all parameters of c-Si modules and I_{SC} of CdTe. Annealing can cause instability of a-Si modules even if kept in an air-conditioned environment, and even more when modules are shipped. Therefore, it must be stated that in the case of thin film modules, calibration cannot be discussed under total exclusion of stability problems. The uncertainty inherent in calibration discussed here refers more or less to purely measurement related uncertainties, which needs to be considered when the magnitude of stability effects is investigated. Awareness is necessary of the possible difference between the results of a module calibration, and the STC parameters relevant for field operation, as will be discussed in more detail in [11].

IV. Conclusion

In this article, we presented results for the uncertainty estimation in Fraunhofer ISE’s CalLab PV Modules for the calibration of crystalline silicon, cadmium telluride and amorphous silicon modules. A new benchmark concerning measurement uncertainty for crystalline silicon was set, which clears the way for reducing uncertainty in production lines as well.

TABLE V
Expanded Uncertainty for different PV Technologies

Expanded Uncertainty (k=2, in %)	I_{SC}	I_{MPP}	V_{OC}	V_{MPP}	$\mathbf{P_{MPP}}$	FF
Standard crystalline silicon	1.3	1.7	0.6	1.2	**1.6**	1.2
Cadmiumtelluride	2.5	2.8	0.7	1.4	**2.9**	1.7
Typical amorphous Silicon (1 p-n junction)	1.4	1.8	0.6	1.3	**1.8**	1.2
CI(G)S	No general uncertainty					

Results for expanded uncertainty (k=2) for different technologies. The corresponding uncertainty for efficiency is 1.9%, 3.1%, and 2.0%, respectively.

Nevertheless, results introduced here represent just the beginning of accurate, comprehensive module characterization, considering the fact that STC measurements are not sufficient for describing module behavior under realistic operating conditions. The optimization of measurement systems at STC must be followed by optimizing measurements at other temperatures and irradiances, in order to enable accurate power rating measurements [45] and to support efforts for accurate energy rating and yield prediction. The extensive, measurement process oriented analysis presented here can easily be adapted for that purpose.

Acknowledgment

We acknowledge Frank Neuberger, Boris Farnung and our collegues from CalLab PV Cells Jochen Hohl-Ebinger and Holger Seifert for helpful discussions and reviewing the manuscript. We thank the whole CalLab PV Modules team for performing the measurements.

References

[1] K. Heidler and J. Beier, "Uncertainty analysis of PV efficiency measurements with a solar simulator - spectral mismatch, non-uniformity and other sources of error," in *Proc. 8th IEEE PVSC*, Florenz, Italy, 1988, pp. 554-559.
[2] K. A. Emery, *et al.*, "Uncertainty analysis of photovoltaic efficiency measurements," in *Proc. 19th IEEE PVSC*, New Orleans, Louisiana, USA, 1987, pp. 153-159.
[3] H. Müllejans, *et al.*, "Analysis and mitigation of measurement uncertainties in the traceability chain for the calibration of photovoltaic devices," *Measurement Science and Technology,* vol. 20, pp. 1-12, Jul 2009.
[4] K. Emery, "Uncertainty Analysis of Certified Photovoltaic Measurements at the National Renewable Energy Laboratory," National Renewable Energy Laboratory (NREL), Golden, CO. NREL/TP-520-45299, Aug 2009.
[5] U. Kräling, *et al.*, "Präzisionsmessungen an PV-Modulen - Anforderungen an die Messtechnik und die Messprozeduren," *Proc.25th Symposium Photovoltaische Sonnenenergie,* Bad Staffelstein, Germany, 2010.
[6] J. Hohl-Ebinger, "Untersuchungen zur hochpräzisen Vermessung der elektrischen Parameter von Solarzellen," Dissertation,

Fachbereich für Physik, Universität Konstanz, Fraunhofer Institut für Solare Energiesysteme (ISE) Freiburg, 2011.
[7] K. Whitfield and C. R. Osterwald, "Procedure for determining the uncertainty of photovoltaic module outdoor electrical performance," *Progress in Photovoltaics: Research and Applications,* vol. 9, pp. 87-102, Mar 2001.
[8] IEC 60904-3 Ed. 2.0, "Photovoltaic devices - Part 3: Measurement principles for terrestrial photovoltaic (PV) solar devices with reference spectral irradiance data," International Electrotechnical Commission (IEC), Geneva, Switzerland, 2008.
[9] Y. Hishikawa*, et al.*, "Round-robin measurement intercomparison of c-Si PV modules among Asian testing laboratories," *Progress in Photovoltaics: Research and Applications*, p. in print, 2012.
[10] M. A. Green*, et al.*, "Solar cell efficiency tables (version 40)," *Progress in Photovoltaics: Research and Applications,* vol. 20, pp. 606-614, Aug 2012.
[11] D. Dirnberger, "Uncertainty in PV Module Measurement - Part II," *To be published,* 2013.
[12] IEC 60904-9 Ed. 2.0, "Photovoltaic devices - Part 9: Solar simulator performance requirements," International Electrotechnical Commission (IEC), Geneva, Switzerland, 2007.
[13] C. R. Osterwald*, et al.*, "The world photovoltaic scale: An international reference cell calibration program," in *Proc. 26th IEEE PVSC*, Anaheim, California, USA, 1997, pp. 1209-1212.
[14] C. R. Osterwald*, et al.*, "The World Photovoltaic Scale: An international reference cell calibration program," *Progress in Photovoltaics,* vol. 7, pp. 287-297, Jul-Aug 1999.
[15] D. L. King*, et al.*, "Measurement precautions for high-resistivity silicon solar cells," in *Proc. 20th IEEE PVSC*, Las Vegas, Nevada, USA, 1988, pp. 555-559.
[16] J. Metzdorf*, et al.*, "Analysis and correction of errors in current-voltage characteristics of solar cells due to transient measurements," in *Proc. 12th EU PVSEC*, Amsterdam, the Netherlands, 1994, pp. 496-499.
[17] T. R. Betts*, et al.*, "Photovoltaic performance measurements in Europe: PV-Catapult round robin tests," in *Proc. 4th IEEE World Conf. Photovoltaic Energy Conversion, Vols 1 and 2*, Waikoloa, Hawaii, 2006, pp. 2238-2241.
[18] W. Herrmann*, et al.*, "Results of the european performance project on development of measurement techniques for thin-film PV modules," in *Proc. 23rd EU PVSEC*, Valencia, Spain, 2008, pp. 2719-2722.
[19] W. Herrmann*, et al.*, "PV module output power characterisation in test laboratories and in the PV industry - results of the european performance project," in *Proc. 25th EU PVSEC / 5th World Conference on Photovoltaic Energy Conversion*, Valencia, Spain, 2010, pp. 3879-3883.
[20] P. Lechner*, et al.*, "Progress in a-Si/a-Si tandem junction thin film solar modules," in *Proc. 24th EU PVSEC*, Hamburg, Germany, 2009, pp. 2390-2393.
[21] D. Dirnberger*, et al.*, "Mastering thin film measurements on a grand scale as a daily routine," in *Proc. 26th European Photovoltaic Solar Energy Conf.*, Hamburg, Germany, 2011, pp. 3261-3266.
[22] S. Winter*, et al.*, "New laser-DSR facility at PTB: concept for a next generation high accuracy primary calibration facility," in *Proc. 26th European Photovoltaic Solar Energy Conf.*, Hamburg, Germany, 2011, pp. 3466-3468.
[23] S. Winter*, et al.*, "Laser-DSR facility at PTB: realization of a next generation high accuracy primary calibration facility," in *Proc. 27th EU PVSEC*, Frankfurt, Germany, 2012, p. in print.
[24] S. Winter*, et al.*, "Primary reference cell calibration at the PTB based on an Improved DSR facility," in *Proc. 16th EU PVSEC*, Glasgow, United Kingdom, 2000.
[25] S. Winter*, et al.*, "The results of the second world photovoltaic scale recalibration," *Proc. 32st IEEE PVSC,* pp. 1011-1014, 2005.
[26] H. Müllejans*, et al.*, "Comparison of traceable calibration methods for primary photovoltaic reference cells," *Progress in Photovoltaics: Research and Applications,* vol. 13, pp. 661-671, Dec 2005.
[27] J. Hohl-Ebinger*, et al.*, "Measuring the spectral distribution of a flash simulator," in *Proc. 22nd EU PVSEC*, Milan, Italy, 2007, pp. 425-428.
[28] IEC 60904-1 Ed. 2.0, "Photovoltaic devices - Part 1: Measurement of photovoltaic current-voltage characteristics," International Electrotechnical Commission (IEC), Geneva, Switzerland, 2006.
[29] ISO/IEC Guide 98-1, "Uncertainty of measurement - Part 1: Introduction to the expression of uncertainty in measurement," International Organization for Standardization (ISO), International Electrotechnical Commission (IEC), Geneva, Switzerland, 2009.
[30] IEC 60904-2 Ed. 2.0, "Photovoltaic devices - Part 2: Requirements for reference solar devices," International Electrotechnical Commission (IEC), Geneva, Switzerland, 2007.
[31] IEC 60904-7 Ed. 3.0, "Photovoltaic devices - Part 7: Computation of the spectral mismatch correction for measurements of photovoltaic devices," International Electrotechnical Commission (IEC), Geneva, Switzerland, 2008.
[32] T. Parkin. (2012). *Python Programming Language - Official Website*. Available: http://www.python.org/
[33] IEC 60891 Ed. 2.0, "Photovoltaic devices - Procedures for temperature and irradiance corrections to measured I-V characteristics," ed: International Electrotechnical Commission (IEC), Geneva, Switzerland, 2009.
[34] M. Gostein and L. Dunn, "Light soaking effects on photovoltaic modules: Overview and literature review," in *Proc. 37th IEEE PVSC*, Seattle, Washington, USA, 2011, pp. 003126-003131.
[35] ISO/IEC Guide 98-3, "Uncertainty of measurement - Part 3: Guide to the expression of uncertainty in measurement (GUM:1995)," International Organization for Standardization (ISO), International Electrotechnical Commission (IEC), Geneva, Switzerland, 2008.
[36] JCGM 100, "Evaluation of measurement data - Guide to the expression of uncertainty in measurement," 2008.
[37] H. Field and K. Emery, "An uncertainty analysis of the spectral correction factor," in *Proc. 23rd IEEE PVSC*, Louisville, Kentucky, USA, 1993, pp. 1180-1187.
[38] J. Hohl-Ebinger and W. Warta, "Uncertainty of the spectral mismatch correction factor in STC measurements on photovoltaic devices," *Progress in Photovoltaics,* vol. 19, pp. 573-579, Aug 2011.
[39] D. L. King*, et al.*, "A sensitivity analysis of the spectral mismatch correction procedure using wavelength-dependent error sources," in *Proc. 22nd IEEE PVSC*, Las Vegas, Nevada, USA, 1991, pp. 459-65.
[40] JCGM 101, "Evaluation of measurement data - Supplement 1 to the "Guide to the expression of uncertainty in measurement" - Propagation of distributions using a Monte Carlo method," 2008.
[41] European Commission Joint Research Centre, "Guidelines for PV Power Measurements in Industry," Publications Office of the European Union, Luxembourg, EUR - Scientific and Technical Research Reports EUR 24359 EN, Apr 2010.
[42] S. Elies*, et al.*, "Influence of row-shading on the performance of PV systems – simulation and measurement," in *Proc. 25th EU PVSEC / 5th World Conf. on Photovoltaic Energy Conversion*, Valencia, Spain, 2010, pp. 4640-4646.
[43] D. Dirnberger*, et al.*, "Uncertainty of field I-V-curve measurements in large scale PV-systems," in *Proc. 25th EU PVSEC / 5th World Conf. on Photovoltaic Energy Conversion*, Valencia, Spain, 2010, pp. 4587-4594.
[44] H. Seifert*, et al.*, "Spectral Influences on Measurement Uncertainty of a-Si/µc-Si Multi-Junction Solar Devices," in *Proc. 26th EU PVSEC*, Hamburg, Germany, 2011.
[45] IEC 61853-1 Ed. 1.0, "Photovoltaic (PV) module performance testing and energy rating - Part 1: Irradiance and temperature performance measurements and power rating," ed: International Electrotechnical Commission (IEC), Geneva, Switzerland, 2011.

Daniela Dirnberger received the diploma in mechanical engineering (Dipl.Ing.) from the Technical University of Dresden in 2008. She is currently working towards her PhD on the topic of thin film module characterization and energy rating. At Fraunhofer ISE's CalLab PV Modules, she is responsible for a team working on improved measurement methods for module characterization.

Ulli Kräling received the diploma in microsystems engineering (Dipl.Ing.) from the Albert-Ludwigs-University of Freiburg in 2008. He is quality manager at CalLab PV Modules.